

# Study of Some Low Temperature Gas-Generating Compositions

Xinliang Mei,<sup>[a]</sup> Hongtao Yang,<sup>[a]</sup> Xiangyu Li,<sup>[a]</sup> Yanchun Li,<sup>[a]</sup> and Yi Cheng<sup>\*,[a]</sup>

**Abstract:** Some low temperature gas-generating compositions, comprised of guanidine nitrate (GN), basic cupric nitrate (BCN), and ferric oxide ( $\text{Fe}_2\text{O}_3$ ), were studied herein. The thermal decomposition properties and burning characteristics of GN/BCN/ $\text{Fe}_2\text{O}_3$  mixtures were investigated by thermogravimetry/differential scanning calorimetry (TG/DSC), burning temperature measurements, automatic calorimetry, and X-ray diffraction (XRD). This study showed that the maximum burning temperature of GN/BCN/ $\text{Fe}_2\text{O}_3$  mix-

ture ( $613^\circ\text{C}$ ) was 31% lower than that of GN/BCN mixture and the corresponding heat of combustion ( $2647\text{ J g}^{-1}$ ) decreased by 15%. When the GN/BCN/ $\text{Fe}_2\text{O}_3$  mixtures were burning,  $\text{Fe}_2\text{O}_3$  did not directly react with GN but with Cu (or CuO), which was produced by reaction between GN and BCN. The combustion process of GN/BCN/ $\text{Fe}_2\text{O}_3$  grains could be divided into four stages: pre-heated, condensed, combustion, and cooling.

**Keywords:** Low temperature • Ferric oxide • Gas-generating agent

## 1 Introduction

In general, the gas-generating agents consist of fuel and oxidant. Guanidine nitrate (GN) has high nitrogen content (49 wt-%) and requires less oxygen [1,2]. Basic cupric nitrate (BCN) can provide more oxygen and has high moisture resistance and high chemistry stability [3–5]. Having the merits of large gas production and rapid combustion rate, the GN/BCN gas-generating agents have been well studied and widely applied [6–9]. In 2010, Yoshino and Miyake [10] investigated the thermal decomposition properties of GN and 1,2,4-triazole-3-one (TO) mixtures. It was proposed that there is an interaction between TO and nitric acid from the dissociation of GN for the thermal decomposition of TO/GN mixtures. Some gas-generating compositions, which consisted of GN, BCN, ammonium perchlorate (AP), and ferric oxide ( $\text{Fe}_2\text{O}_3$ ), were studied [11]. When the gas-generating agent was characterized in a closed bomb test, both the maximum pressure and the rate of pressure rise were measured as characterized parameters. Accordingly, the optimum composition was obtained.

Some non-toxic metal oxides (copper oxide, iron oxide, and alumina) could be used as oxidizers in the gas-generating composition. Shingo Date et al. researched guanidinium 1,5-bis-1H-tetrazolate (G15B) and metal oxide mixtures as the candidate of gas-generating agent. G15B/ $\text{Fe}_2\text{O}_3$  mixture was the most insensitive among G15B/metal oxide mixtures during the drop hammer test [12].  $\text{Fe}_2\text{O}_3$  could reduce the pressure exponent and enable the composition to sustain combustion at or near atmospheric pressure. Higher amounts of  $\text{Fe}_2\text{O}_3$  (10% or more) would improve ballistic properties in certain propellant compositions [13,14].

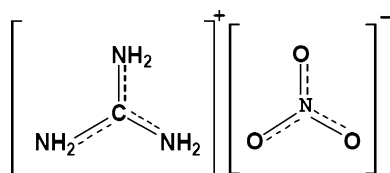
The calculated value of adiabatic flame temperature of GN/BCN mixture is about 1900 K [15]. In order to achieve a gas-generating agent which has lower combustion temperature and better combustion characteristics, some non-toxic metal oxides (copper oxide, iron oxide, and alumina) were selected to replace a part of BCN as the second oxidant. In this report,  $\text{Fe}_2\text{O}_3$  was chosen as the second oxidant for replacement of part of BCN in the GN/BCN mixture. The thermal decomposition behaviors of GN/BCN/ $\text{Fe}_2\text{O}_3$  mixtures were investigated by thermogravimetry/differential scanning calorimetry (TG/DSC). The combustion characteristics of GN/BCN/ $\text{Fe}_2\text{O}_3$  mixtures were investigated by burning temperature measurement, heat of combustion measurement and analysis of the combustion residue.

## 2 Experimental

### 2.1 Reagents

The purity of GN (Sanming Coffe Fine Chemical Industrial Co., Ltd) was 98.26%, and the average particle size was  $5.52\text{ }\mu\text{m}$ . The copper and nitrate contents of BCN (Sanming Coffe Fine Chemical Industrial Co., Ltd) were 52.83% and 24.58%, respectively. The 50% accumulative size (D50) was  $1.63\text{ }\mu\text{m}$ . The average particle size of  $\text{Fe}_2\text{O}_3$  (Shanghai Chan-

[a] X. Mei, H. Yang, X. Li, Y. Li, Y. Cheng  
School of Chemical Engineering  
Nanjing University of Science and Technology  
Xiaolingwei 200, Nanjing 210094, P. R. China  
\*e-mail: chengyi20@aliyun.com

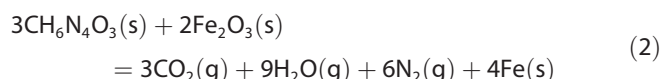
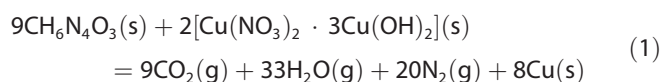


Guanidine nitrate

Figure 1. Molecular structure of GN.

gnan Chemical, 98%) was 5.02  $\mu\text{m}$ . Molecular structure of GN is shown in Figure 1.

Reagents were mixed by carefully sieving through a 200 mesh sieve (74  $\mu\text{m}$ ) three times. Samples were prepared by mixing a stoichiometric composition based on Equation (1) and Equation (2). Table 1 shows the compositions of the mixtures.



## 2.2 Apparatus and Methods

### 2.2.1 Measurement of Thermal Decomposition Behavior

TG/DSC experiments were performed with a NETZSCH STA449C apparatus at a heating rate of 5  $\text{Kmin}^{-1}$  from 100  $^{\circ}\text{C}$  to 400  $^{\circ}\text{C}$  in a high-purity argon atmosphere (20  $\text{mLmin}^{-1}$ ). Each sample was weighed about 1.0 mg and placed in an alumina crucible (80  $\mu\text{L}$ ) with a perforated cover for the TG/DSC measurements. Before testing, all mixtures were stored in a vacuum oven at 65  $^{\circ}\text{C}$  for 3 h to remove water.

### 2.2.2 Measurement of Burning Characteristics

The heat of combustion was measured with a Hunan YouXin YX-ZR Type automatic calorimeter in a nitrogen atmosphere at 3.0 MPa. Benzoic acid was used to calibrate the thermal capacity of automatic calorimeter. GN/BCN/ $\text{Fe}_2\text{O}_3$  mixtures were weighed at about 3.0 g. Each of the

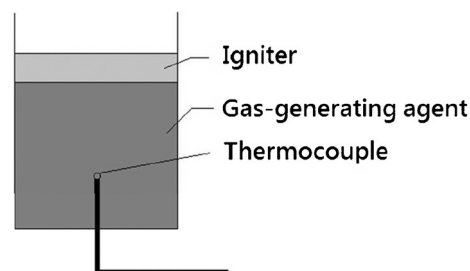


Figure 2. Experimental setup for measuring burning temperature.

mixtures was tested three times, and the average heat of combustion was calculated. After measuring the heat of combustion, the solid residue was analyzed by X-ray diffraction with a Bruker D8 ADVANCE.

The burning temperature was measured in air at the standard atmospheric pressure. As shown in Figure 2, the gas-generating agent and igniter were loaded in the combustion chamber in turn. A 1 mm diameter WRe5/WRe26 thermocouple was vertically inserted into the gas-generating grain on the axes of the direction of combustion and was connected to a dynamic signal analyzer (Industrialacs Computer 2000).

## 3 Results and Discussion

### 3.1 Thermal Decomposition Behavior

Figure 3 shows the results of thermal analysis for the GN/BCN mixture (1#), GN/BCN/ $\text{Fe}_2\text{O}_3$  mixtures (2#–6#) and the GN/ $\text{Fe}_2\text{O}_3$  mixture (7#). The temperatures at 5% mass loss ( $T_{\text{TGS}5\%}$ ), the temperature of endothermic peak ( $T_{\text{p1}}$ ), the temperature of first exothermic peak ( $T_{\text{p2}}$ ), the temperature of second exothermic peak ( $T_{\text{p3}}$ ), and the temperature of third exothermic peak ( $T_{\text{p4}}$ ) are listed in Table 2.

The main mass loss temperatures of three GN/BCN/ $\text{Fe}_2\text{O}_3$  mixtures are in the range of 150–250  $^{\circ}\text{C}$ . One endothermic peak (about 175  $^{\circ}\text{C}$ ) and three exothermic peaks (about 190  $^{\circ}\text{C}$ , 200  $^{\circ}\text{C}$ , and 240  $^{\circ}\text{C}$  separately) could be observed. Increasing the mass ratio of  $\text{Fe}_2\text{O}_3$ , the heat flow of the first exothermic peaks decreased, and the third exothermic peak disappeared gradually. Comparing the TG curves of GN/BCN/ $\text{Fe}_2\text{O}_3$  mixtures with that of the GN/ $\text{Fe}_2\text{O}_3$  mixture,

Table 1. Compositions of the GN/BCN/ $\text{Fe}_2\text{O}_3$  mixtures.

| Sample | Mass fraction of $\text{Fe}_2\text{O}_3$<br>in oxidizing agent [%] | GN/BCN/ $\text{Fe}_2\text{O}_3$ |                   |
|--------|--|---------------------------------|-------------------|
|        |  | Mol ratio                       | Mass ratio        |
| 1#     | 0  | 81.82/18.18/0                   | 53.35/46.65/0     |
| 2#     | 10   | 78.95/15.79/5.26                | 53.35/41.99/4.66  |
| 3#     | 20   | 76.28/13.56/10.16               | 53.36/37.32/9.32  |
| 4#     | 30   | 73.78/11.48/14.74               | 53.36/32.66/13.98 |
| 5#     | 40   | 71.45/9.52/19.03                | 53.37/27.99/18.64 |
| 6#     | 50   | 69.26/7.69/23.05                | 53.38/23.32/23.30 |
| 7#     | 100  | 60.05/0/39.95                   | 53.40/0/46.60     |

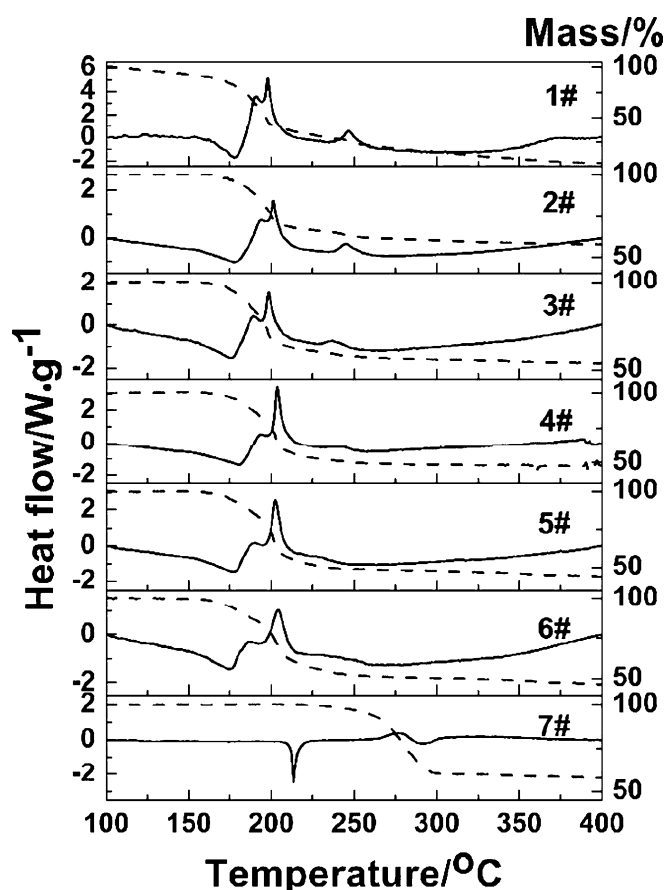


Figure 3. DSC/TG curves of GN/BCN/Fe<sub>2</sub>O<sub>3</sub> mixtures.

Table 2. Results of the thermal analysis of the GN/BCN/Fe<sub>2</sub>O<sub>3</sub> mixtures.

| Sample | $T_{\text{TGS}} [^{\circ}\text{C}]$ | $T_{\text{p1}} [^{\circ}\text{C}]$ | $T_{\text{p2}} [^{\circ}\text{C}]$ | $T_{\text{p3}} [^{\circ}\text{C}]$ | $T_{\text{p4}} [^{\circ}\text{C}]$ |
|--------|-------------------------------------|------------------------------------|------------------------------------|------------------------------------|------------------------------------|
| 1#     | 127.6                               | 177.4                              | 190.8                              | 197.5                              | 246.3                              |
| 2#     | 180.3                               | 178.2                              | 194.4                              | 201.2                              | 244.5                              |
| 3#     | 175.2                               | 176.5                              | 189.6                              | 198.2                              | 236.2                              |
| 4#     | 178.1                               | 180.2                              | 194.1                              | 203.5                              | 243.1                              |
| 5#     | 174.7                               | 177.0                              | 189.6                              | 202.6                              | –                                  |
| 6#     | 174.4                               | 174.2                              | 186.9                              | 204.1                              | –                                  |
| 7#     | 257.9                               | 213.5 <sup>a)</sup>                | 278.0                              | –                                  | –                                  |

a) Temperature of the GN melting peak.

the onset reaction temperature of the GN/Fe<sub>2</sub>O<sub>3</sub> mixture (257.9 °C) is higher than the end reaction temperature of GN/BCN/Fe<sub>2</sub>O<sub>3</sub> mixtures (about 250 °C). It demonstrates that Fe<sub>2</sub>O<sub>3</sub> does not directly react with GN in GN/BCN/Fe<sub>2</sub>O<sub>3</sub> mixtures. It is possible that Fe<sub>2</sub>O<sub>3</sub> reacts with Cu (or CuO) produced by the redox reaction between GN and BCN (Section 3.2 will discuss the reaction of GN/BCN/Fe<sub>2</sub>O<sub>3</sub> mixtures).

The thermal behavior (DSC curves) of all GN/BCN/Fe<sub>2</sub>O<sub>3</sub> mixtures is almost similar to that of the GN/BCN mixture, even though the onset temperature ( $T_{\text{TGS}}$ ) of GN/BCN/

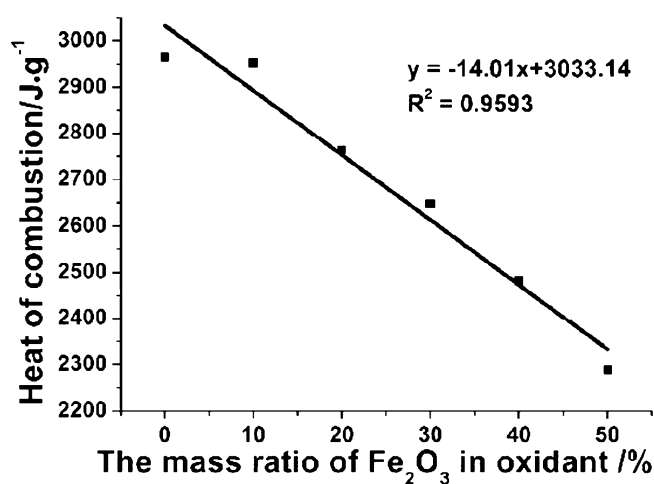


Figure 4. Heat of combustion for GN/BCN/Fe<sub>2</sub>O<sub>3</sub> mixtures.

Fe<sub>2</sub>O<sub>3</sub> mixtures are higher by 50 °C than that of the GN/BCN mixture. It indicates that the thermal reaction processes of GN/BCN/Fe<sub>2</sub>O<sub>3</sub> mixtures are supposed to be the same with that of the GN/BCN mixture, but the thermal stability of GN/BCN/Fe<sub>2</sub>O<sub>3</sub> mixtures are higher than that of the GN/BCN mixture at a heating rate of 5 K min<sup>-1</sup>.

### 3.2 Combustion Reaction

The relationship between the heat of combustion and the mass ratio of Fe<sub>2</sub>O<sub>3</sub> in oxidizing agents is displayed in Figure 4. The heat of combustion decreases with increasing mass ratio of Fe<sub>2</sub>O<sub>3</sub> in the mixtures. And a good linear relationship is demonstrated with  $R^2$  value larger than 0.95. From this relationship, it is assumed that the heat of combustion of GN/Fe<sub>2</sub>O<sub>3</sub> mixture is 1401 J g<sup>-1</sup>, whereas the calculated value is 1447.4 J g<sup>-1</sup> with relative error of 3.2% [9].

Figure 5 shows the X-ray diffraction pattern of the combustion residue for the GN/BCN/Fe<sub>2</sub>O<sub>3</sub> mixtures. The pattern of Cu is confirmed in the residue of mixture without Fe<sub>2</sub>O<sub>3</sub> (sample 1#). When the mass ratio of Fe<sub>2</sub>O<sub>3</sub> in the oxidant is 10–30% (sample 2#, 3#, and 4#), FeCu<sub>4</sub> and CuFe<sub>2</sub>O<sub>4</sub> are confirmed in the combustion residues. In addition to FeCu<sub>4</sub> and CuFe<sub>2</sub>O<sub>4</sub>, FeO is also detected in the combustion residues of sample 5# and 6#. It is indicated that the combustion reactions of GN/BCN/Fe<sub>2</sub>O<sub>3</sub> mixtures are insufficient.

Because Fe<sub>2</sub>O<sub>3</sub> does not directly react with GN in GN/BCN/Fe<sub>2</sub>O<sub>3</sub> mixtures, Fe<sub>2</sub>O<sub>3</sub> probably reacts with Cu (or CuO) which is produced by burning reaction between GN and BCN. When the Fe<sub>2</sub>O<sub>3</sub> mass content in oxidant is 10–30% (sample 2#, 3#, and 4#), Equation (3) and Equation (4) could describe the reaction mechanism. As the mass ratio of Fe<sub>2</sub>O<sub>3</sub> in the GN/BCN/Fe<sub>2</sub>O<sub>3</sub> mixtures increases, the peak intensity of CuFe<sub>2</sub>O<sub>4</sub> in the XRD curves ( $2\theta = 36^{\circ}$  is more especially obvious) gradually increases. When Fe<sub>2</sub>O<sub>3</sub> mass content in the oxidant is increased to 40–50%, Equation (5) is the main reaction between Cu and Fe<sub>2</sub>O<sub>3</sub>. Thus, the

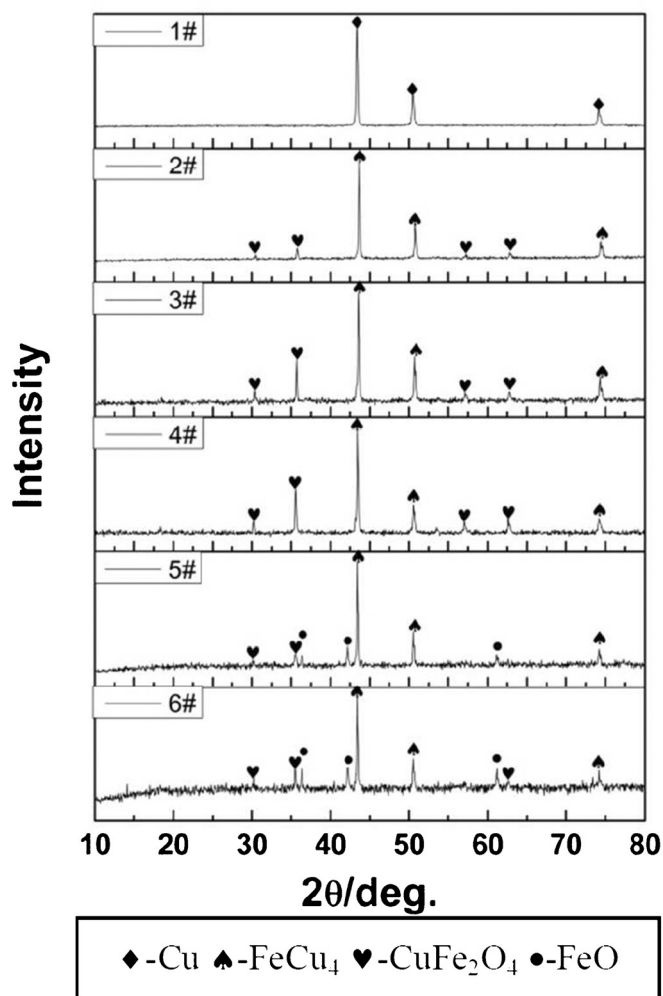
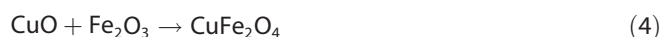


Figure 5. XRD pattern of the combustion residue in the GN/BCN/ $\text{Fe}_2\text{O}_3$  mixtures.

peaks intensities of  $\text{CuFe}_2\text{O}_4$  and  $\text{FeO}$  ( $2\theta = 36^\circ$  and  $37^\circ$ ) in the XRD curves increase together.



The typical temperature-time curve for the combustion of GN/BCN/ $\text{Fe}_2\text{O}_3$  gas generating agent is given in Figure 6. The combustion process of GN/BCN/ $\text{Fe}_2\text{O}_3$  mixture is divided into preheating stage, condensed stage, combustion stage and cooling stage. Firstly, the grain is preheated to  $215^\circ\text{C}$  [16] which is the melting temperature of GN and the end of pre-ignition reaction. Next, the temperature goes up to a certain point rapidly (condensed stage). After the certain temperature, the temperature increases gradually to the maximum point (combustion stage). Finally, the temperature starts to drop, which is probably caused by the

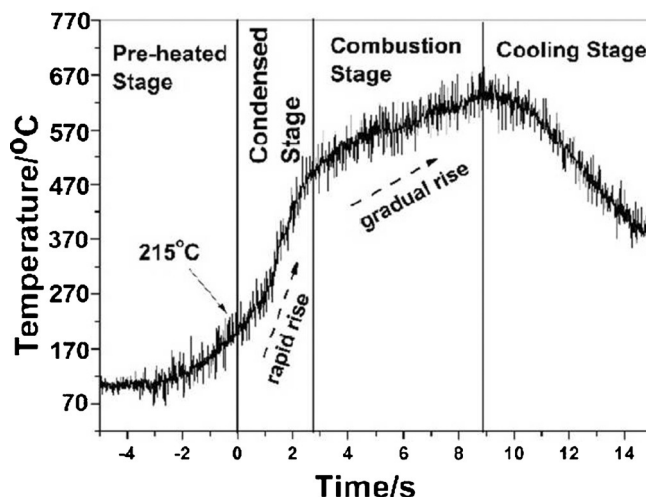


Figure 6. Temperature-time curve for gas generating agents.

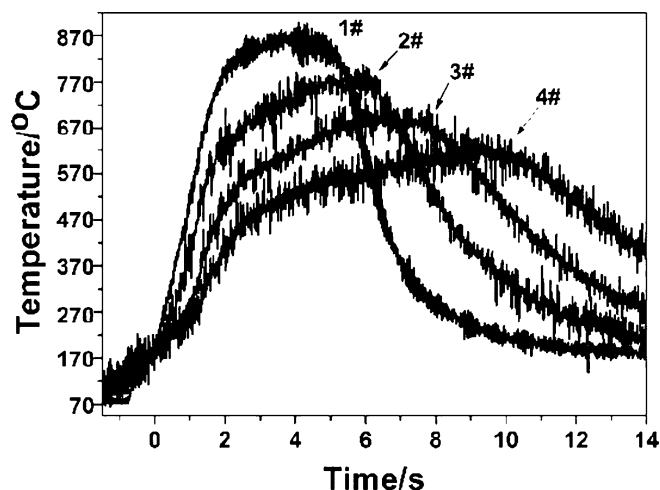


Figure 7. Temperature-time curves for GN/BCN/ $\text{Fe}_2\text{O}_3$  mixtures.

cooling of combustion residue [17]. It is probable that the condensed stage with a dramatic increase in temperature is caused by a large heat release at  $150\text{--}250^\circ\text{C}$  in DSC.

Figure 7 shows the temperature-time curves for different GN/BCN/ $\text{Fe}_2\text{O}_3$  mixtures. The duration of combustion stage and the maximum temperature are listed in Table 3. Samples 5#–7# did not burn in air at the standard atmospheric pressure. Increasing  $\text{Fe}_2\text{O}_3$  in GN/BCN/ $\text{Fe}_2\text{O}_3$  mixtures, the

Table 3. Duration of the combustion zone and the maximum temperature.

| Sample | Condensed stage [s] | Combustion stage [s] | Maximum temperature [ $^\circ\text{C}$ ] |
|--------|---------------------|----------------------|--|
| 1#     | 1.80                | 2.58                 | 893                                      |
| 2#     | 1.73                | 4.55                 | 788                                      |
| 3#     | 1.87                | 5.62                 | 693                                      |
| 4#     | 1.90                | 6.97                 | 613                                      |

duration of condensed stage was not significantly different, while the duration of combustion stage increased remarkably. The increasing duration of combustion stage indicates that the combustion rate of GN/BCN/Fe<sub>2</sub>O<sub>3</sub> mixture is slower. In addition, it is shown that the decreasing maximum burning temperature is caused by the decreasing of heat of combustion (Figure 4).

## 4 Conclusions

Based on the investigation of the thermal decomposition properties and the burning process of GN/BCN/Fe<sub>2</sub>O<sub>3</sub> mixtures, the following conclusions were drawn.

(1) When Fe<sub>2</sub>O<sub>3</sub> was added in place of some BCN in GN/BCN mixture, the thermal stability increased and the combustion rate decreased. Meanwhile, the maximum burning temperature decreased and the heat of combustion decreased.

(2) When the GN/BCN/Fe<sub>2</sub>O<sub>3</sub> mixture was burning, Fe<sub>2</sub>O<sub>3</sub> did not directly react with GN and probably reacted with Cu (or CuO) which was produced by burning reaction between GN and BCN.

(3) A large heat release at 150–250 °C in DSC caused the dramatic temperature rise at the condensed stage.

## References

- [1] Y. Yamato, *Gas Generating Composition*, US Patent 2009/0211671, Falls Church, VA, USA, **2009**.
- [2] J. C. Oxley, J. L. Smith, S. Naik, J. Moran, Decompositions of Urea and Guanidine Nitrates, *J. Energ. Mater.* **2009**, *27*, 17–39.
- [3] H. R. Blomquist, A. M. Helmy, W. P. Sampson, M. G. Mangum, *Cool Burning Gas Generating Material for a Vehicle Occupant Protection Apparatus*, US Patent 6,875,295, TRW Inc., Lyndhurst, OH, USA, **2005**.
- [4] J. Wu, S. Tomiyama, *Gas Generating Composition for Inflator Containing Melamine Cyanurate*, US Patent 2010/0078098 A1, Falls Church, VA, USA, **2010**.
- [5] S. Tomiyama, *Gas Generating Composition*, US Patent 8,034,133 B2, Daicel Chemical Industries Ltd., Osaka, Japan, **2011**.
- [6] K. Kitayama, S. Tomiyama, *Gas Generating Composition*, US Patent 7,887,650 B2, Daicel Chemical Industries Ltd., Sakai-Shi, Japan, **2011**.
- [7] K. Kitayama, S. Tomiyama, *Rare Earth Compound Containing Gas Generating Composition*, US Patent 7,833,365 B2, Daicel Chemical Industries Ltd., Sakai-Shi Osaka, Japan, **2010**.
- [8] J. Wu, *Gas Generating Composition*, US Patent 8,137,771 B2, Daicel Chemical Industries Ltd., Osaka, Japan, **2012**.
- [9] X. Mei, Y. Cheng, Y. Li, X. Zhu, S. Yan, X. Li, Thermal Decomposition Properties of Guanidine Nitrate and Basic Cupric Nitrate, *J. Therm. Anal. Calorim.* **2013**, *114*, 131–135.
- [10] S. Yoshino, A. Miyake, Thermal Decomposition Properties of 1,2,4-Triazole-3-one and Guanidine Nitrate Mixtures, *J. Therm. Anal. Calorim.* **2010**, *102*, 513–516.
- [11] Y. D. Seo, S. H. Chung, J. J. Yoh, Automotive Airbag Inflator Analysis using the Measured Properties of Modern Propellants, *Fuel* **2011**, *90*, 1395–1401.
- [12] S. Date, T. Sugiyama, N. Itadzu, S. Nishi, Burning Characteristics and Sensitivity Characteristics of Some Guanidinium 1,5'-Bis-1H-Tetrazolate/Metal Oxide Mixtures as Candidate Gas Generating Agent, *Propellants Explos. Pyrotech.* **2011**, *36*, 51–56.
- [13] B. K. Wheatley, *Metal Oxide Containing Gas Generating Composition*, US Patent 6,274,064, Atlantic Research Corporation, Gainesville, VA, USA, **2001**.
- [14] B. K. Wheatley, *Metal Oxide Containing Gas Generating Composition*, US Patent 6,156,230, Atlantic Research Corporation, Gainesville, VA, USA, **2000**.
- [15] J. Wu, *Gas Generating Composition*, CN Patent 1556782A, Daicel Chemical Industries Ltd., Osaka, Japan, **2004**.
- [16] R. Meyer, J. Köhler, A. Homburg, *Explosives*, 5th ed., Wiley-VCH, Weinheim, **2002**, p. 156.
- [17] Y. Miyata, K. Hasue, A Thermal Decomposition Model of Aminoguanidinium 5,5'-Azobis-1H-tetrazolate and the Effect of Pressure and Particle Size on the Rate of Decomposition, *Propellants Explos. Pyrotech.* **2009**, *34*, 498–505.

Received: August 4, 2014

Revised: October 30, 2014

Published online: December 10, 2014